IEEE Access
Multidisciplinary | Rapid Review | Open Access Journal

Received March 26, 2020, accepted April 7, 2020, date of publication April 13, 2020, date of current version May 4, 2020.

Digital Object Identifier 10.1109/ACCESS.2020.2987607

Charging Strategy Unifying Spatial-Temporal Coordination of Electric Vehicles

JIALEI ZHANG[1,2], (Member, IEEE), YUNQING PEI[2], (Member, IEEE), JIAMING SHEN[2], (Student Member, IEEE), LAILI WANG[2], (Senior Member, IEEE), TAO DING[2], (Senior Member, IEEE), AND SEN WANG[2], (Graduate Student Member, IEEE)

[1]Department of electric power engineering, Shanxi University, Taiyuan 030006, China
[2]School of Electrical Engineering, Xi'an Jiaotong University, Xi'an 710049, China

Corresponding author: Laili Wang (llwang@mail.xjtu.edu.cn)

ABSTRACT This paper focuses on how to make a charging guidance for urgent charging electric vehicles (EVs) to fast charging stations. To avoid charging overload in the spatial-temporal scale and excessive waiting time for EV users, a charging guidance strategy based on the virtual service range is proposed. Considering the mutual influence among EVs' charging selections, the proposed strategy can unify the temporal shift and spatial shift of the charging load into the same time scale to control rather than other works only do the temporal shift. Specifically, the proposed strategy has two stages: the charging arrangement and the spatial-temporal shift. The charging arrangement stage is to determine whether an EV can be allowed to charge at a certain time and a given charging station while the spatial-temporal shift stage is to regulate the charging time or charging location. Besides, a bucketsort-based algorithm is proposed to solve the formulated problem in the charging arrangement stage. Finally, three scenarios have been designed to demonstrate the feasibility of the proposed strategy and the performance of the presented algorithm is compared with the other decentralized algorithms.

INDEX TERMS Charging load, driving time, electric vehicle, spatial-temporal, waiting time.

I. INTRODUCTION

The widespread adoption of electric vehicles (EVs) can help to reduce air pollution, greenhouse gas emissions, and health risks [1]. However, the uncoordinated charging of EVs may jeopardize the security and reliability of the power grid, especially in terms of peak load. Taking Guangdong province in China as an example, due to the lack of charging management, its peak load will increase by at least 1.64% in 2020 [2]. Therefore, charging management technologies are needed.

A. RESEARCH PROBLEM

Generally, EV users have two charging cases: destination charging and urgent charging [3], [4]. For destination charging EVs, charging location is definite, e.g., home, workplace, and public parking lots etc., and parking duration is relatively long. Therefore, the charging rate or charging start time can be regulated to shift the collective charging load peak in the time domain [5]–[7]. For the urgent charging EVs, when and where to charge are indeterminate. They need to be decided by EV users. However, EV users' charging decisions can be affected by various factors. Typically, if too many EVs coincidentally gather at the same charging station, some EVs may need to wait a long time to charge and the local overload of the feeder connected by the charging station may become more serious. In other words, there exists the mutual influence among EVs' charging selections. These decisions may collectively affect the spatial-temporal distribution of the total charging load and bring a part of EVs undesired time cost without suitable coordination. As shown in Fig. 1, the users of EV A, EV B, and EV C may most possibly select the closer charging station CS1 instead of CS2. When the surplus charging durations of the charging EV1, EV2, EV3, and EV4 are 30 min and that of the charging EV5 is 10 min, EV A does not need to wait, EV B waits for 4 min and EV C waits for 22 min to charge at CS1. Therefore, the better choice for EV C should be CS2 under the consideration of the other two EVs' selections. Although it may cause more driving time, the total time cost can be saved. In this work, we focus on the two questions about urgent charging EVs.

The associate editor coordinating the review of this manuscript and approving it for publication was Xiaosong Hu.

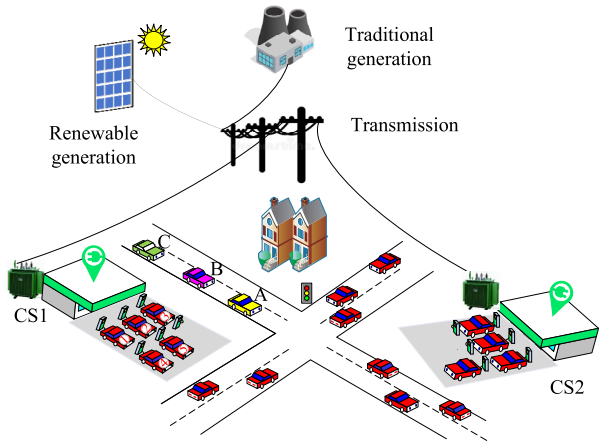

FIGURE 1. Example of the mutual influence among EVs charging selections: the driving time to CS1 for EV A,EV B, and EV C is 5 min, 6 min, and 8 min, and the driving time to CS2 for EV A,EV B, and EV C is 12 min, 13 min, and 15 min.

- For a fleet of EVs, how to avoid charging overload in the spatial-temporal scale?
- For an EV, how to guide it to a fast charging station without undesired waiting time?

B. RELATED WORKS

1) SPATIAL-TEMPORAL MODEL FOR EV CHARGING LOAD

In order to model the spatial-temporal characteristics of EV charging load, some approaches have been presented, e.g., the origin-destination (OD) approach [8], [15], trip chain [9], [10], agent-based approach [11], Markov chain approach [12], [13], stochastic approach [14], queuing theory [15], multiple agents approach [16], and mobile crowdsensing data approach [17]–[19]. In [8], the OD analysis was used to model the EV mobility, i.e., the travel distance of each EV within a day and the time (or the location) that EVs start charging. The trip chain method was developed based on the national household trip survey (NHTS) data [9] or the Naive Bayes model [10]. According to the prediction of EV users' day-ahead driving behavior, [11] proposed an agent-based centralized spatial-temporal coordination charging strategy. However, the accuracy of the prediction will significantly affect the charging decision. The Markov chain model was developed by using geospatial maps [12] or real-time closed-circuit television data [13]. In addition, [14] proposed a two-stage stochastic model, which considers customers' satisfaction, driving patterns, real-time market prices, and network operation indices. In [15], the OD analysis was developed to obtain all the EV charging points, and a capacity determination model based on the queuing theory was proposed to determine the capacity of each EV charging station.

Unlike the aforementioned works, some studies only focus on the spatial-temporal distribution of the charging load of plug-in electric taxis (PETs) rather than that of all types of EVs. In [16], a multiple-agent framework was proposed to simulate the operation of related players. Reference [17] presented a mobile crowdsensing system to forecast the charging behavior of PET based on both the historical and real-time data of PET, rather than the historical data of PET (e.g., from the global positioning system (GPS) [18], [19]) or the historical data of the inner-combustion-engine vehicles (e.g., from NHTS).

2) CHARGING GUIDANCE FOR AN EV TO A FAST CHARGING STATION

Existing literature on a charging guidance for an EV to a fast charging station can be divided into two categories: pricing [20]–[23] and non-pricing [24]–[29].

Pricing methods consider a pricing competition among fast charging stations to attract EVs indirectly, so pricing methods emphasis on how to make a price and build a response-to-price model of EV users. In [21], a non-cooperative game was presented to set the price for charging station, while multiple evolutionary games were formulated to guide EVs to choose fast charging stations based on the price from the upper stage. Reference [22] presented a multileader-multifollower Stackelberg game model, in which leaders (i.e., charging stations) announce their prices in stage I and followers (i.e., EVs) make their charging selections in stage II. In [23], a super modular game model was developed to analyze the competitive price of multiple fast charging stations with renewable power generators. In comparison, [23] pointed out the charging choices of EVs were dependent on each other, which was ignored by [21] and [22].

Non-pricing approaches directly offer charging selections for EV users based on the knowable information, so non-pricing approaches emphasis on how to integrate the data from different sources. Reference [24] introduced a charging navigation system that revised the traffic distance to an electrical distance to consider the power system operation information. In [25], both the traffic system and the power system were united into a time term by the charging guidance system. According to the predictions, including traffic flow, average speed, travel time and charging time, [26] proposed a navigation system to discover the shortest route. In [27], a hierarchical navigation strategy based on dynamic traffic and temperature data was proposed. The upper layer was the charging time selection while the lower layer was the charging route selection. Reference [28] formulated an interdisciplinary second order cone programming model that optimizes PEVs' driving paths and charging locations. Reference [29] made a charging recommendation based on both the fast charging stations' conditions and a global knowledge of EV users' charging selections. Unlike [24]–[28], [29] considered the mutual influence among multiple EVs' charging selections. However, [29] can only make the coordination of multiple EVs' charging selections in a single charging station and cannot conduct the coordination among charging stations.

C. SUMMARY

Our main contributions are summarized as follows. (1) To unify the spatial shift and temporal shift of EVs into the same time scale, a virtual service range (VSR) concept is

proposed. Based on the VSR principle, a charging guidance strategy is designed. The proposed strategy can complete the temporal shift of EVs for a single charging station and spatial shift of EVs among multiple charging stations, in contrast to similar works that do not consider the mutual influence among multiple EVs' charging selections. (2) The VSR-based charging strategy has two stages: the charging arrangement and the spatial-temporal shift. To solve the formulated problem in the charging arrangement stage, a decentralized bucketsort-based algorithm is proposed. (3) The VSR-based charging strategy can save time cost for EV users and avoid local overload for power grid. Compared with the other decentralized algorithms, the bucketsort-based algorithm can guarantee a high optimality rate under a lower data size of communication.

The rest of this paper is organized as follows. In Section II, the charging guidance strategy for urgent charging EVs to a fast charging station is formulated based on the VSR principle. In Section III, a bucketsort-based algorithm is proposed. In Section IV, various simulations are carried out. Finally, conclusions are drawn in Section V.

II. SYSTEM DESCRIPTION AND PROBLEM FORMULATION

A. SYSTEM DESCRIPTION

The charging guidance system is designed for the two problems in Section I-A. When a moving EV needs to recharge urgently, the EV user will beforehand send a charging requirement to the desired charging station. Then, the selected charging station determines the charging time that the EV can be allowed to charge. If the waiting time exceeds the acceptable limit of EV user, the EV will be regulated to charge at another charging station.

As illustrated in Fig. 2, the charging guidance system comprises three parts: EV terminals, the charging station operators (COs), and the distribution system operator (DO). In this architecture, the communications between an EV and its corresponding CO, between the COs and DO, and among the COs are required. The first two are needed by a decentralized algorithm in Section III while the third is for the charging location regulation.

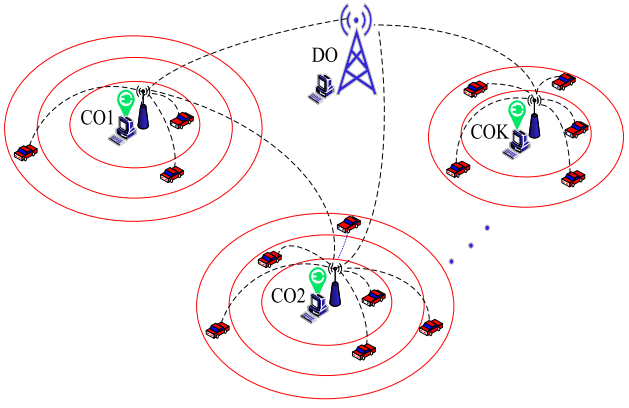

FIGURE 2. Communication structure of the VSR-based charging strategy.

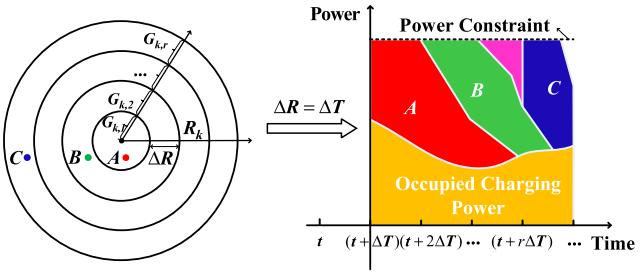

FIGURE 3. Schematic diagram of the time-power transform based on the VSR.

B. PROBLEM FORMULATION

By the given system, the collective coordination of EV charging time reflects the temporal shift of the charging load for each charging station, while the aggregate coordination of EV charging location exhibits the spatial shift of the charging load among the charging stations. During the coordinating progress, a part of EVs may need to be temporally regulated while another portion may need to be spatially transferred. Therefore, the charging guidance strategy should be able to address spatial shift and temporal shift at the same time, i.e., how to unify the temporal shift and spatial shift of the charging load into the same time scale to control. In order to handle the challenge, we propose a VSR concept.

1) VIRTUAL SERVICE RANGE

We denote the EV that sends a charging requirement to a fast charging station as the unscheduled EV (USEV). Let $i = 1, 2, \ldots, N_k$ and $k = 1, 2, \ldots, K$ denote USEVs and charging stations, respectively. We consider coordinating USEVs charging in terms of their driving time, which can be obtained from some applications or equipment, e.g., Google map, Baidu map, and Gaode map, or EV build-in energy management system. How to calculate the driving time by combing with the related factors, e.g., travel distance, driving pattern, driving speed, traffic flow, and weather, is not within the scope of this paper.

Let $T_{i,k}^{driv}$ denote the time that USEV i drives to the charging station k. Assume that USEVs near the charging station k form a VSR, which is a circle scope with the center of the charging station's geographical position and with the radius of the maximum USEVs driving time. The service radius for the charging station k is defined as

$$R_k = \max\{T_{1,k}^{driv}, T_{2,k}^{driv}, \cdots, T_{i,k}^{driv}, \cdots\}, \quad i = 1, 2, \cdots N_k, \quad k = 1, 2, \cdots K. \tag{1}$$

As displayed in Fig. 3, the service radius R_k is discretized into a number N_R of equal radius intervals ΔR, which further makes the service range divided into a number N_R of annular bands $G_{k,r}$. Annular band $G_{k,r}$ for the charging station k is defined as

$$G_{k,r} = [(r-1)\Delta R, r\Delta R], \quad r = 1, 2, \cdots, N_R. \tag{2}$$

Then, the USEVs within the annular band $G_{k,r}$ can be judged by

$$(r-1)\Delta R < T_{i,k}^{driv} \le r\Delta R, \quad \forall i \in US_{k,r},\ i=1,2,\cdots N_{k,r}. \tag{3}$$

Let $US_{k,r}$ denote the set of USEVs within the annular band $G_{k,r}$. The number of $US_{k,r}$ is denoted as $N_{k,r} = |US_{k,r}|$ and the total number of USEVs is $\sum_{r=1}^{N_R} N_{k,r} = N_k$. The lower subscript of the specification of USEVs in $US_{k,r}$ is marked as (i,k,r).

As indicated in Fig. 3, ΔR is set to be equal to the control interval ΔT. This setting is a key of the proposed VSR principle. It can bring three advantages: (i) USEVs among different annular bands of the same charging station can be supplied the reasonable charging time, which can ensure USEVs arrive at the designated charging station on time; (ii) USEVs among the same annular band of different charging stations can be coordinated at the same time; (iii) The charging load for USEVs at the annular band can be transformed and reflected in the time-power coordinate, which is a link of traffic system and power system.

2) THE PROPOSED CHARGING GUIDANCE STRATEGY

The VSR-based charging strategy is formulated into two stages: the charging arrangement and the spatial-temporal shift. The charging arrangement stage is to decide whether an EV can be allowed to charge at a certain time and a given charging station. The spatial-temporal shift stage is to regulate the charging time or charging station.

a: STAGE ONE: CHARGING ARRANGEMENT

On a first-come-first-served basis, the COs will supply the charging service for the USEVs that arrive earlier, which is quantified as the charging priority $H_{i,k,r}$

$$H_{i,k,r} = \frac{1}{T_{i,k,r}^{driv}}. \tag{4}$$

For a single charging station, the number of USEVs that can be accommodated by the selected charging station should be limited by the available charging power, which is expressed as

$$\sum_{i=1}^{N_{k,r}} P_{i,k,r}^{char} \cdot x_{i,k,r}^{char} \le P_k - \sum_{j=1}^{M_k} P_{j,k}, \quad \forall i \in US_{k,r},\ \forall j \in OP_k. \tag{5}$$

where $P_{i,k,r}^{char}$ represents the charging power required by USEV i. $x_{i,k,r}^{char}$ is a binary decision variable for USEV i. P_k is the amount of electrical energy supplied by the charging station k. $j = 1,2,\ldots,M_k$ represents the occupied charging piles. $P_{j,k}$ represents the output power of the occupied charging piles. OP_k represents the set of the occupied charging piles. For K charging stations, the total charging load of USEVs cannot form the undesired peak load, which is expressed as

$$\sum_{k=1}^{K}\sum_{i=1}^{N_{k,r}} P_{i,k,r}^{char} \cdot x_{i,k,r}^{char} \le P_{ref} - \sum_{k=1}^{K}\sum_{j=1}^{M_k} P_{j,k}, \quad \forall i \in US_{k,r}, \quad \forall j \in OP_k. \tag{6}$$

where P_{ref} reflects the power instruction from economic optimization or operation constraints of distribution system, e.g., the active power of the optimal power flow, or the stochastic renewable generation, e.g., photovoltaic generation.

Hence, the objective of the charging arrangement problem is to maximize the cumulative charging priority while fulfilling two power constraints, which is formulated as

$$\begin{aligned} &\max \sum_{k=1}^{K}\sum_{i=1}^{N_{k,r}} H_{i,k,r}^{char} \cdot x_{i,k,r}^{char} \\ &\text{s.t. (5), (6),}\ x_{i,k,r}^{char} = \{1,0\}, \\ &\quad \forall i \in US_{k,r}, \quad \forall j \in OP_k,\ k = 1,2,\cdots K, \\ &\quad \forall r \in [1, N_R]. \end{aligned} \tag{7}$$

According to the decision variable $x_{i,k,r}^{char}$, USEV i may have two arrangements, which is expressed as

$$\begin{cases} x_{i,k,r}^{char} = 1, & \forall i \in CA_{k,r}, \\ x_{i,k,r}^{char} = 0, & \forall i \in TS_{k,r}. \end{cases} \tag{8}$$

$CA_{k,r}$ represents the set of the USEVs that obtain the charging allowance. $TS_{k,r}$ represents the set of the USEVs that do not obtain the charging allowance and need to be spatially or temporally shifted. For the USEVs in $CA_{k,r}$, the charging arrangement is estimated as

$$\begin{cases} T_{i,k,r}^{wait} = F_{i,k,r}^{temp} \cdot \Delta T, \\ T_{i,k,r}^{char} = t + (r + F_{i,k,r}^{temp})\Delta T, \\ \text{chariging location: CS}k. \end{cases} \tag{9}$$

where $T_{i,k,r}^{wait}$ denotes the estimated time that USEV i may wait for an idle charger after arriving at a fast charging station, $T_{i,k,r}^{char}$ denotes the estimated time that USEV i is connected into an idle charger and starts charging, and $F_{i,k,r}^{temp}$ represents the number of temporal shift USEV i has experienced. As displayed in (9), the USEV i in $CA_{k,r}$ is allowed to start charging at the time interval $t + (r + F_{i,k,r}^{temp})\Delta T$ and at the fast charging station k.

b: STAGE TWO: SPATIAL-TEMPORAL SHIFT

In order to make the USEVs in $TS_{k,r}$ obtain a charging allowance, they are temporally shifted or spatially shifted according to the related constraints. The first constraint is that the estimated waiting time exceeds the longest waiting time, which is formulated as

$$(F_{i,k,r}^{temp} + 1) \cdot \Delta T \ge T_{i,k,r}^{limi}. \tag{10}$$

where $T_{i,k,r}^{limi}$ is the longest waiting time tolerated by USEV user.

The second constraint is that the current state of charge (SOC) of the USEV can support a spatial shift [25], which is formulated as

$$Q_{i,k,r}(SOC^{curr}_{i,k,r} - SOC^{\min}_{i,k,r}) \geq D_{i,k^*} \cdot V_{i,k,r}. \quad (11)$$

where Q_i represents the battery capacity of USEV i. $SOC^{curr}_{i,k,r}$ denotes the current SOC of the battery in USEV i. $SOC^{min}_{i,k,r}$ denotes the minimum SOC to avoid the excessive discharge. D_{i,k^*} denotes the route distance from USEV i to the charging station k^*. $V_{i,k,r}$ denotes the average consumption electricity per kilometer. k^* is the candidate charging station that USEV i will be spatially shifted from the charging station k.

The third constraint is that the total time cost maintains a minimum, which is expressed as (12). In other words, the sum of the driving time and the estimated waiting time when USEV i recharges at the charging station k is higher than the driving time T^{driv}_{i,k^*} that USEV i drives to the candidate charging station k^*.

$$T^{driv}_{i,k,r} + (F^{temp}_{i,k,r} + 1) \cdot \Delta T > T^{driv}_{i,k^*} + \alpha \quad (12)$$

α denotes an incentive factor to change charging location for EV users, which is a tradeoff between electric energy cost and time cost. The candidate charging station k^* can be selected by the requirement that the driving time T^{driv}_{i,k^*} is the shortest to the charging stations whose available service capacity is idle.

$$k^* = \min\{T^{driv}_{i,1}, T^{driv}_{i,2}, \cdots, T^{driv}_{i,k^*}, \cdots | SV_{k^*} = 1\}. \quad (13)$$

The available service capacity SV_k is denoted as

$$SV_k = \begin{cases} 1, & \text{if } 0 < \dfrac{N_k}{(M^{total}_k - M_k)} < 1, \\ 0, & \text{if } 1 < \dfrac{N_k}{(M^{total}_k - M_k)} < 1 + \beta, \\ -1, & \text{if } 1 + \beta < \dfrac{N_k}{(M^{total}_k - M_k)}. \end{cases} \quad (14)$$

$SV_k = 1, 0$, or -1 respectively represents that the serviceable capacity is idle, normal, or busy. β is the dynamic margin of the serviceable capacity. M^{total}_k is the total number of the charging piles equipped by the charging station k.

Therefore, for the USEVs in $TS_{k,r}$, the charging arrangement is formulated as

$$\begin{cases} F^{spat}_{i,k,r} = 1, F^{temp}_{i,k,r} = 0, & \text{if (10), (11), and (12) hold,} \\ F^{spat}_{i,k,r} = 0, F^{temp}_{i,k,r} = F^{temp}_{i,k,r} + 1, & \text{otherwise.} \end{cases} \quad (15)$$

where $F^{spat}_{i,k,r} = 1$ represents the flag that USEV i needs to be spatially shifted. As displayed in (15), once the three constraints in (10)-(12) are satisfied simultaneously, the USEV will be spatially shifted.

c: IMPLEMENTATION OF STRATEGY

As shown in Fig. 4, the scheduling process of the VSR-based charging strategy is described as follows.

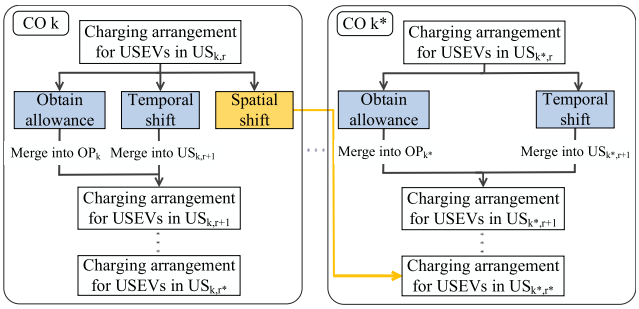

FIGURE 4. Scheduling process of the VSR-based charging strategy.

(i) At time slot t, each CO receives information from the DO and USEVs. According to the scheduling sequence $(US_{k,1}, US_{k,2}, \ldots, US_{k,r}, US_{k,r+1}, \ldots, US_{k,N_R})$, the COs handle USEVs in order.

(ii) For USEVs among the same annular band of different charging stations, the COs can jointly decide their charging arrangements, including obtain a charging allowance (i.e., $i \in CA_{k,r}$), a temporal shift (i.e., $F^{temp}_{i,k,r} > 0, i \in TS_{k,r}$), or a spatial shift (i.e., $F^{spat}_{i,k,r} = 1, i \in TS_{k,r}$).

(iii) For USEVs with charging allowances, they are merged into OP_k. For the temporal shift USEVs in $TS_{k,r}$, they are reformulated into USEVs in $US_{k,r+1}$ to further take participate in the next charging arrangement.

(iv) Repeat the process (ii) and (iii) until all the USEVs are handled.

(v) If there exists the spatial shift USEVs in the process (i)-(iv), the spatial shift USEVs in $TS_{k,r}$ are reformulated into USEVs in US_{k^*,r^*} (where r^* can be determined by (3)) and the strategy returns to the process (i)-(iv) to handle all the USEVs until there are no the spatial shift USEVs.

III. DECENTRALIZED ALGORITHM

The formulated problem (7) is a 0-1 linear program (0-1 LP). Based on the linear-programming relaxation, a branch-and-bound algorithm is generally applied to solve the 0-1 LP. However, it is a centralized method, which requires the information of all USEVs is transmitted to a central controller (e.g., the DO) to handle. With the increasing penetration of EVs, the centralized algorithm is not suitable because of heavy computation and communication. Therefore, a decentralized algorithm is considered, i.e., the related data of the USEVs only need to be transmitted to the corresponding COs rather than the DO.

Inspired by the existing consensus-based algorithm [5] and the alternating direction method of multipliers (ADMM-based) algorithm [30], we propose a decentralized bucketsort-based algorithm. The optimality analysis of the proposed algorithm is given by Appendix.

The following are the detail steps of the proposed algorithm. To express simply, we make the definitions $\tilde{P}_k = P_k - \sum_{j=1}^{M_k} P_{j,k}$, and $\tilde{P}_{ref} = P_{ref} - \sum_{k=1}^{K} \sum_{j=1}^{M_k} P_{j,k}$.

Input: $H_{i,k,r}$, $P^{char}_{i,k,r}$, $\tilde{P}_k$, and $\tilde{P}_{ref}$.
Output: $x^{char}_{i,k,r}$.
Algorithm: Bucketsort-Based Algorithm
Step 1: In terms of the charging priority per unit power $U_{i,k,r}=(H_{i,k,r}/P^{char}_{i,k,r})$, CO k sorts USEVs in $US_{k,r}$ in a descending order,

$$I_k = \{U_{1,k,r}, U_{2,k,r}, \cdots, U_{i,k,r}, \cdots, U_{(N_{k,r}),k,r}\},$$
$$U_{i,k,r} \geq U_{(i+1),k,r} \tag{16}$$

Step 2: In order to satisfy the power constraint in (5), when $\sum_{i=1}^{N_{k,r}} P^{char}_{i,k,r} > \tilde{P}_k$, I_k is truncated as $\tilde{I}_k$.

$$\tilde{I}_k = \{U_{1,k,r}, U_{2,k,r}, \cdots, U_{i,k,r}, \cdots, U_{(\tilde{N}_{k,r}),k,r}\},$$
$$\sum_{i=1}^{\tilde{N}_{k,r}} P^{char}_{i,k,r} \leq \tilde{P}_k \leq \sum_{i=1}^{(\tilde{N}_{k,r})+1} P^{char}_{i,k,r}. \tag{17}$$

The decision variables of the truncated elements are determined as $x^{char}_{i,k,r} = 0, \forall i \in [(\tilde{N}_{k,r}) + 1, N_{k,r}]$. To guarantee the power constraint in (6), the steps 3-5 decentrally make a bucket sort, which is a recursive process and needs very little data exchange between the COs and the DO.

Step 3: In the τ^{th} recursion, CO k classifies USEVs in $\tilde{I}_k$ into M different buckets $B^{\tau}_{k,m}(m = 1, 2, \ldots, M)$ according to $U_{i,k,r}$. If (18) is established, USEV i is assigned into the bucket m, i.e., $i \in B^{\tau}_{k,m}$.

$$max^{\tau}_U + m\frac{max^{\tau}_U - min^{\tau}_U}{M} < U_{i,k,r} < max^{\tau}_U + (m-1)\frac{max^{\tau}_U - min^{\tau}_U}{M}$$
$$\forall i \in [1, \tilde{N}_{k,r}], \quad \forall m \in [1, M] \tag{18}$$

The total power of USEVs in each bucket is calculated as

$$sum^{\tau}_{k,m} = \sum P^{char}_{i,k,r}, \quad i \in B^{\tau}_{k,m}. \tag{19}$$

Then, the COs transmit $sum^{\tau}_{k,m}$ $(m = 1, 2, \ldots, M)$ to the DO.

Step 4: The DO makes the judgment according to the power constraint in (6).

(i) If M^{τ}_{th} fulfills the requirement (20.a), $M^{\tau}_{th} = 1$.

$$sum^{(\tau-1)}_{DO} + \sum_{m=1}^{1}\sum_{k=1}^{K} sum^{\tau}_{k,m} > \tilde{P}_{ref} \tag{20a}$$

(ii) If M^{τ}_{th} fulfills the condition (20.b), $M^{\tau}_{th} \in (1, M]$.

$$sum^{(o-1)}_{DO} + \sum_{m=1}^{M^{\tau}_{th}}\sum_{k=1}^{K} sum^{\tau}_{k,m} > \tilde{P}_{ref} > sum^{(\tau-1)}_{DO} + \sum_{m=1}^{M^{\tau}_{th}-1}\sum_{k=1}^{K} sum^{\tau}_{k,m} \tag{20b}$$

(iii) M^{τ}_{th} is returned to the COs. The allowable charging power for all the charging station sum^{τ}_{DO} is updated as

$$sum^{\tau}_{DO} = sum^{(\tau-1)}_{DO} + \sum_{m=1}^{M^{\tau}_{th}-1}\sum_{k=1}^{K} sum^{\tau}_{k,m}, \quad \forall M^{\tau}_{th} \in (1, M] \tag{21}$$

Step 5: In terms of the received M^{τ}_{th}, CO k can make the following decisions for USEVs in $\tilde{I}_k$.

(i) If $M^{\tau}_{th} = 1$,

$$x_{i,k,r} = 0, \quad \forall i \in B^{\tau}_{k,m}, \ \forall m \in [2, M] \tag{22a}$$

(ii) If $M^{\tau}_{th} \in (1, M)$,

$$\begin{cases} x_{i,k,r} = 1, & \forall i \in B^{\tau}_{k,m}, \ \forall m \in [1, M^{\tau}_{th} - 1] \\ x_{i,k,r} = 0, & \forall i \in B^{\tau}_{k,m}, \ \forall m \in [M^{\tau}_{th} + 1, M] \end{cases} \tag{22b}$$

(iii) If $M^{\tau}_{th} = M$,

$$x_{i,k,r} = 1, \quad \forall i \in B^{\tau}_{k,m}, \ \forall m \in [1, M^{\tau}_{th} - 1] \tag{22c}$$

(iv) Except for the bucket M^{τ}_{th}, USEVs in other buckets have acquired the decisions $x^{char}_{i,k,r}$. When the number of recursion τ is not larger than the maximum recursion τ^{max}, we need to return to the ***Step 3***, replace $\tilde{I}_k$ by the bucket M^{τ}_{th}, and refresh $max^{(\tau+1)}_U$ and $min^{(\tau+1)}_U$ as

$$\begin{cases} max^{(\tau+1)}_U = max^{\tau}_U - (M^{\tau}_{th} - 1)\dfrac{max^{\tau}_U - min^{\tau}_U}{M} \\ min^{(\tau+1)}_U = max^{\tau}_U - M^{\tau}_{th}\dfrac{max^{\tau}_U - min^{\tau}_U}{M} \end{cases} \tag{23}$$

IV. CASE STUDIES

To verify the feasibility of the VSR-based charging strategy, we design three scenarios: a charging arrangement without the spatial-temporal shift, a charging arrangement with the temporal shift, and a charging arrangement with the spatial-temporal shift.

A. PARAMETER SETTINGS AND ASSUMPTIONS

We assume that there are 5 fast charging stations. For each fast charging station, the number of annular bands N_R, the radius interval ΔR, dynamic margin δ, the total number of charging piles M^{total}_k are set as 8, 5 min, 0.5 and 120, respectively. The power instruction from the distribution system P_{ref} is uniformly distributed between 5000 kW and 12000 kW. The supplied power of charging station P_k is uniformly distributed between 1300 kW and 2500 kW. The output power of charging piles is 20 kW. The number of USEVs uniformly varies over 0 to 120. For USEVs, the driving time $T^{driv}_{i,k,r}$ and the current SOC $SOC^{curr}_{i,k,r}$ are picked uniformly at random from $[5(r-1), 5r]$ $(r = 1, 2, \ldots, 8)$ and [0.2, 0.5], respectively. The charging power $P^{char}_{i,k,r}$, the battery capacity Q_i, the average energy consumption $V_{i,k,r}$ and the minimum SOC $SOC^{min}_{i,k,r}$ are 20 kW, 60 kWh, 0.18 kWh/km and 0.15 [25].

B. SIMULATION SCENARIOS

1) SCENARIO I: A CHARGING ARRANGEMENT WITHOUT THE SPATIAL-TEMPORAL SHIFT

The aggregate load curve of 5 fast charging stations and the corresponding situation of the fast charging station 1 (CS1) are displayed in Fig. 5. It can be observed that there are two cases: the total required power is lower than the total available power, i.e., $\sum_{k=1}^{K}\sum_{i=1}^{N_{k,r}} P_{i,k,r}^{char} \le P_{ref} - \sum_{k=1}^{K}\sum_{i=1}^{M_k} P_{j,k}$, and the total required power is higher than the total available power, i.e., $\sum_{k=1}^{K}\sum_{i=1}^{N_{k,r}} P_{i,k,r}^{char} > P_{ref} - \sum_{k=1}^{K}\sum_{i=1}^{M_k} P_{j,k}$.

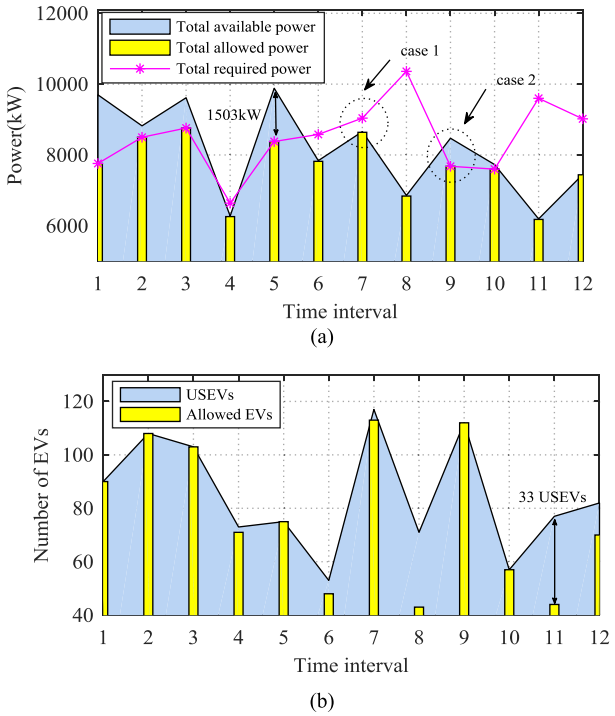

FIGURE 5. Aggregate charging load and the number of EVs in Scenario I.

As the case 1 occurs, the total allowed power, i.e., $\sum_{k=1}^{K}\sum_{i=1}^{N_{k,r}} P_{i,k,r}^{char} x_{i,k,r}^{char}, x_{i,k,r}^{char} = 1$, is equal to the total required power, e.g., time interval 1, 2, 3, 5, 9, and 10 in Fig. 5(a). It means that the charging demand of all USEVs at the corresponding time interval can be satisfied, e.g., at time interval 1 of Fig. 5(b), all the 90 USEVs are allowed to charge at CS1. When the case 2 arises, the total allowed power closely tracks the total available power to acquire available power as much as possible, e.g., time interval 4, 6, 7, 8, 11, and 12 in Fig. 5(a). Overall, for the two cases, the total allowed power never exceeds the total available power, i.e., the undesired peak load can be effectively avoided. Therefore, the charging arrangement part of the VSR-based charging strategy can determine the charging permission of USEVs as well as restrict the aggregate charging overload. However, some problems cannot be handled by the charging arrangement part. In the case 1, the available power is not fully utilized, e.g., at the time interval 5, 1503 kW active power may be curtailed in Fig. 5(a). In the case 2, a part of USEVs cannot obtain the charging permissions, e.g., at time interval 11 of Fig. 5(b), 33 USEVs for CS1 do not obtain the charging permission.

2) SCENARIO II: A CHARGING ARRANGEMENT WITH THE TEMPORAL SHIFT

As illustrated in Fig. 3, the charging load for USEVs at the corresponding annular band can be transformed and reflected in the time-power coordinate. Thus, the annular band r in Scenario II and Scenario III is equivalent to the time interval $r\Delta T$. Based on Scenario I, the temporal shift of the charging load for CS1 is simulated by two cases. In the case 1, we simulate the service capacity of CS1 is normal, i.e., $SV_1 = 1$. As shown in Fig. 6(a), at time interval 5, 780 kW of 2320 kW required power, i.e., $\sum_{i=1}^{N_{k,r}} P_{i,k,r}^{char}, k = 1$, is limited by 1540 kW available power, i.e., $P_k - \sum_{j=1}^{M_k} P_{j,k}, k = 1$.

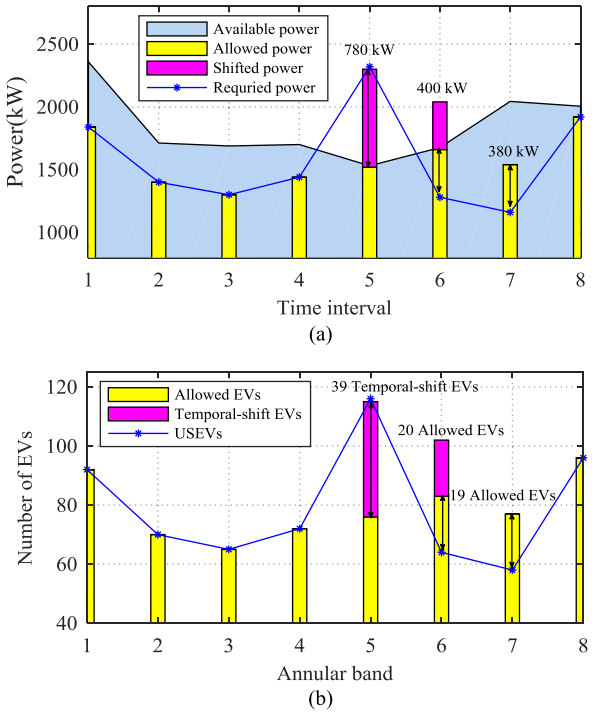

FIGURE 6. Charging load and the number of EVs for the case 1 of Scenario II.

However, by temporal shift, 400 kW of 780 kW shifted power, i.e., $\sum_{i=1}^{N_{k,r}} P_{i,k,r}^{char} - (P_k - \sum_{j=1}^{M_k} P_{j,k}), k = 1$, is transmitted from time interval 5 to 6, and 380 kW of 780 kW shifted power is shifted from time interval 5 to 7. It is observed by that the allowable power (i.e., $\sum_{i=1}^{N_{k,r}} P_{i,k,r}^{char} x_{i,k,r}^{char}, x_{i,k,r}^{char} = 1, k = 1$) adds 400 kW and 380 kW on the required power at time interval 6 and 7, respectively. It is indicated that temporal shift of charging load can improve the utilization of the available power.

Simultaneously, as displayed in Fig. 6(b), for annular band 5, 77 allowed USEVs do not need to wait to charge at time interval 5, 20 of 39 temporal shift EVs (TSEVs) need to wait for 5 min to charge at time interval 6, and the other

19 of 39 TSEVs need to wait for 10 min to charge at time interval 7. By temporal shift, all the USEVs can obtain the charging allowances.

In the case 2, we simulate the service capacity of CS1 is busy, i.e., $SV_1 = -1$. As illustrated in Fig. 7(a) and (b), at time interval 1, because 360 kW available power is far lower than 2200 kW required power, 28 TSEVs are delayed 5 min to charge, 18 TSEVs are delayed 10 min, 17 TSEVs are delayed 15 min, 17 TSEVs are delayed 20 min, and the other 12 TSEVs are delayed 25 min. However, the overlong waiting time cannot be accepted by EV users.

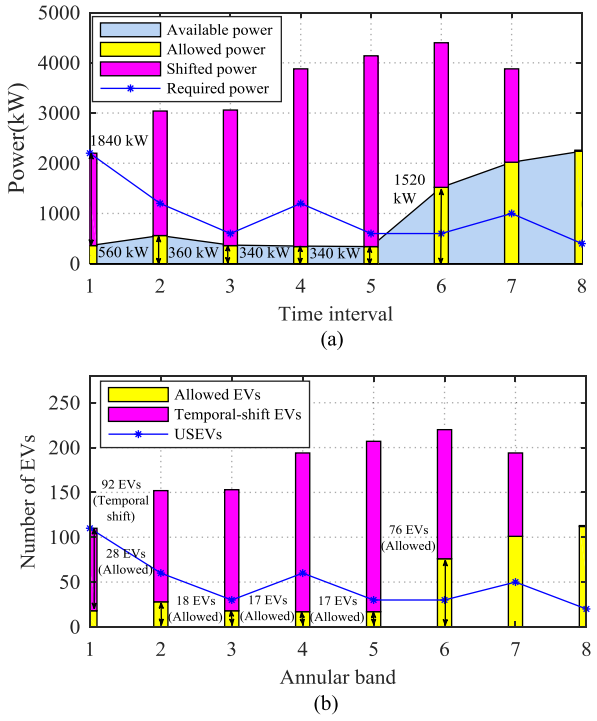

FIGURE 7. Charging load and the number of EVs for the case 2 of Scenario II.

3) SCENARIO III: A CHARGING ARRANGEMENT WITH THE SPATIAL-TEMPORAL SHIFT

We assume that the longest waiting time tolerated by USEV user $T^{limi}_{i,k,r}$ and the incentive factor α are 20 min and 5 min. The service capacity of 5 charging stations are respectively $SV_1 = -1, SV_2 = 1, SV_3 = 1, SV_4 = 1, SV_5 = 0$. As illustrated in Fig. 8(a), the estimated waiting time of 7 TSEVs in CS1 has exceeded out of 20 min at time interval 5. As displayed in Table I, for these 7 TSEVs, we assume the driving time $T^{driv}_{i,5}(i = 1, 2, 3 \ldots 7)$ and the route distance $D_{i,5}$ are selected randomly from [10 min, 15 min] and [5 km, 18 km], respectively. According to the constraints in (10)-(12), except "EV3", the other 6 TSEVs can be spatially shifted to CS5. Because the current SOC of "EV3" cannot support a spatial shift and has to make a temporal shift in CS1 continuously. As displayed in Fig. 8(b), at annular

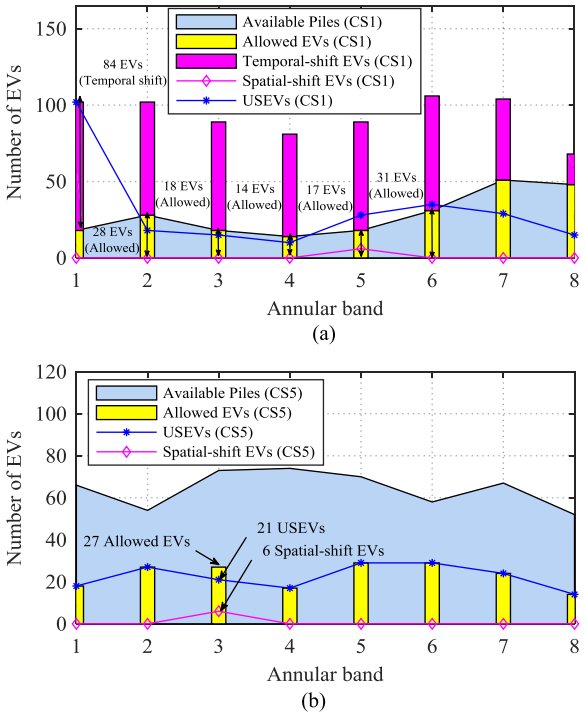

FIGURE 8. The number of EVs in Scenario III.

band 3, there are 27 allowed EVs, which is 6 higher than 21 USEVs. The extra 6 allowed EVs come from CS1.

Besides, for these 7 TSEVs in CS1, the time cost by only temporal shift (i.e., "Time cost (TS)") and the time cost by spatial-temporal shift (i.e., "Time cost (STS)") are summarized in Table 1. It can be seen, for EV1, EV2, EV4, EV5, EV6, and EV7 users, their time cost can be saved at least 11 min by spatial shift.

TABLE 1. Time cost of the 7 TSEVs in CS1.

EV No.	$T^{driv}_{i,1,1}$ (min)	$SOC^{curr}_{i,1,1}$	$T^{driv}_{i,5}$ (min)	$D_{i,5}$ (km)	Time cost (TS)	Time cost (STS)	Time cost savings
EV1	5	0.25	11	9	30	11	19
EV2	5	0.3	14	13	30	14	16
EV3	4	0.2	13	17	29	/	/
EV4	4	0.4	12	6	29	12	17
EV5	5	0.2	11	12	30	11	19
EV6	4	0.2	10	7	29	10	11
EV7	5	0.3	15	8	30	15	15

To make a general comparison of spatial-temporal shift and temporal shift, we assume that the longest waiting time $T^{limi}_{i,k,r}$, the incentive factor α, and $(T^{driv}_{i,k,r,} - T^{driv}_{i,k*})$ are 5 min, 0 min and 5 min, and the current SOC of USEVs can support a spatial shift. The average waiting time of the allowed EVs by temporal shift and spatial-temporal shift is summarized into Table 2. As illustrated in Table 2, the average waiting time of the allowed EVs by temporal shift is constantly Table 1 accumulating and far beyond the limit of the longest waiting

time $T^{limi}_{i,k,r}$, while the average waiting time of the allowed EVs by spatial-temporal shift keeps under the limit of the longest waiting time $T^{limi}_{i,k,r}$. Thus, the overlong waiting time can be avoided for EV users by spatial shift. In Table 2, $(x)_t$ represents the number of EVs at the time t.

TABLE 2. Comparison of Temporal shift and Spatial-Temporal Shift.

Strategy	Time interval	t=1	t=2	t=3	t=4	t=5
	USEV	21	21	21	21	21
	Available Pile	10	10	10	10	10
Temporal shift	Allowed EV	$(10)_1$	$(10)_1$	$\begin{cases}(1)_1,\\(9)_2\end{cases}$	$(10)_2$	$\begin{cases}(2)_2,\\(8)_3\end{cases}$
	Temporal shift EV	$(11)_1$	$\begin{cases}(1)_1,\\(21)_2\end{cases}$	$\begin{cases}(12)_2,\\(21)_3\end{cases}$	$\begin{cases}(2)_2,\\(21)_3,\\(21)_4\end{cases}$	$\begin{cases}(13)_3,\\(21)_4,\\(21)_5\end{cases}$
	Average waiting time (min)	0	5	5.5	10	11
Spatial-Temporal shift	Allowed EV	$(10)_1$	$(10)_1$	$(10)_2$	$(10)_3$	$(10)_4$
	Temporal shift EV	$(11)_1$	$(21)_2$	$(21)_3$	$(21)_4$	$(21)_5$
	Spatial shift EV	0	$(1)_1$	$(11)_2$	$(11)_3$	$(11)_4$
	Average waiting time (min)	0	5	5	5	5

C. ALGORITHM ANALYSIS

Unlike the ADMM-based algorithm, both the bucketsort-based and the consensus-based algorithms can effectively guarantee the power constraint in (6). Besides, the bucketsort-based algorithm needs much less the data size of communication than the consensus-based algorithm, which is displayed in Table 3. Taking a 20000 EVs and 10 COs case as an example, when other conditions are the same, the consensus-based algorithm needs extra $\tau^{con} = 70$ iterations with the neighbor COs to reach a consensus.

TABLE 3. Data size of algorithms.

Bucketsort-based		
Communication Ports	Send to COs	Receive from COs
EVs	$2N_k$	N_k
DO	τK	τMK
Consensus-based[5]		
Communication Ports	Send to COs	Receive from COs
EVs	$2N_k$	1(broadcast)
COs	$\tau^{con}(\tau MK/2)$	$\tau^{con}(\tau MK/2)$

According to the optimality analysis of Appendix, the convergence degree of the bucketsort-based algorithm is also related to recursion times τ and the number of buckets M. ε denotes the accuracy of charging priority per unit power. In our simulation, $U_{i,k,r}$ is normalized, max^1_U and min^1_U are initialized as 100 and 0. If $\varepsilon = 0.1$, considering a tradeoff between data size of communication and the convergence degree, we set $M = 4$. As shown in Fig. 9, considering the case 2 in Scenario I, when the ratio of total required power and total available power is 40%, 50%, 60%, 70%, 80%, and 90%, the optimality rate $(1 - g)$ of the bucketsort-based algorithm becomes approximate to 1 as recursion times τ increases and can go beyond 0.99 at the 5th recursion.

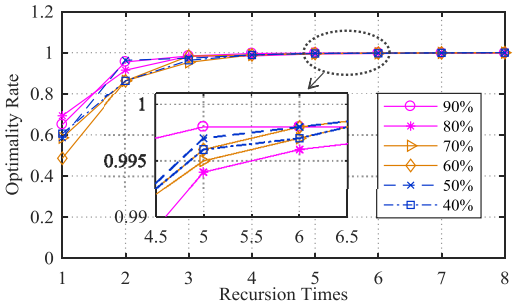

FIGURE 9. Relationship of optimality rate and recursion times.

V. CONCLUSION

In this paper, the VSR-based charging guidance strategy is proposed to benefit both the power system and the EV users. With the introduction of VSR, the proposed strategy can achieve the spatial-temporal shift of EVs rather than only make the temporal coordination for a single charging station. Additionally, the decentralized bucketsort-based algorithm is presented to solve the formulated problem in the charging arrangement stage. From the simulations, it has been demonstrated that the proposed charging strategy and the decentralized algorithm have advantages in terms of saving time cost, alleviating local overload and reducing data size of communication.

APPENDIX

Proposition: When there is the only one USEV in the bucket $M^{\tau max}_{th}$, the optimality of the bucketsort-based algorithm is equivalent to that of the centralized algorithm. Otherwise, there exists an optimality gap.

Proof: Let $(\cdot)^{Buck}$ and $(\cdot)^{Cent}$ mark the variables of the bucketsort-based algorithm and the centralized algorithm, respectively. According to *Step 3-5*, sum^{τ}_{DO} increases by $\sum_{m=1}^{M^{\tau}_{th}-1}\sum_{k=1}^{K} sum^{\tau}_{k,m}$ recursively and approaches $\tilde{P}_{ref}$ asymptotically. Hence, the power constraint in (6) is rewritten as

$$\sum_{k=1}^{K}\sum_{i=1}^{\tilde{N}_{kr}} P^{char}_{i,k,r}\cdot x^{char}_{i,k,r} = part^{Buck}_{cons1} + part^{Buck}_{cons2} < \tilde{P}_{ref}, \quad (24a)$$

$$part^{Buck}_{cons1} = \sum_{m=1}^{M^1_{th}-1}\sum_{k=1,i\in B^1_{k,m}}^{K} P^{char}_{i,k,r} + \sum_{m=1}^{M^2_{th}-1}\sum_{k=1,i\in B^2_{k,m}}^{K} P^{char}_{i,k,r} \cdots + \sum_{m=1}^{M^{\tau}_{th}-1}\sum_{k=1,i\in B^{\tau}_{k,m}}^{K} P^{char}_{i,k,r}, \quad (24b)$$

$$part^{Buck}_{cons2} = \sum_{m=1}^{M^{\tau}_{th}}\sum_{k=1,i\in B^{\tau}_{k,m}}^{K} P^{char}_{i,k,r}\cdot x^{char}_{i,k,r}. \quad (24c)$$

Based on $part_{cons1}^{Buck}$ and $part_{cons2}^{Buck}$, the objective value of bucketsort-based algorithm is deduced as

$$\max^{Buck} = \sum_{k=1}^{K}\sum_{i=1}^{\tilde{N}_{kr}} H_{i,k,r}^{char}\cdot x_{i,k,r}^{char} = part_{obj1}^{Buck} + part_{obj2}^{Buck}, \tag{25a}$$

$$part_{obj1}^{Buck} = \sum_{m=1}^{M_{th}^{1}-1}\sum_{k=1,i\in B_{k,m}^{1}}^{K} H_{i,k,r}^{char} + \sum_{m=1}^{M_{th}^{2}-1}\sum_{k=1,i\in B_{k,m}^{2}}^{K} H_{i,k,r}^{char} \cdots + \sum_{m=1}^{M_{th}^{\tau}-1}\sum_{k=1,i\in B_{k,m}^{\tau}}^{K} H_{i,k,r}^{char}, \tag{25b}$$

$$part_{obj2}^{Buck} = \sum_{m=1}^{M_{th}^{\tau}}\sum_{k=1,i\in B_{k,m}^{\tau}}^{K} H_{i,k,r}^{char}\cdot x_{i,k,r}^{char}. \tag{25c}$$

Assume that bucket sort is also applied in centralized algorithm. Unlike bucketsort-based algorithm, bucketsort of centralized algorithm needs to be implemented by a centralized method. Hence, the power constraint in (6) is rewritten as

$$\sum_{k=1}^{K}\sum_{i=1}^{\tilde{N}_{kr}} P_{i,k,r}^{char}\cdot x_{i,k,r}^{char} = part_{cons1}^{Cent} + part_{cons2}^{Cent} < \tilde{P}_{ref}, \tag{26a}$$

$$part_{cons1}^{Cent} = \sum_{m=1}^{M_{th}^{1}-1}\sum_{i\in B_{m}^{1}} P_{i,k,r}^{char} + \sum_{m=1}^{M_{th}^{2}-1}\sum_{i\in B_{m}^{2}} P_{i,k,r}^{char} \cdots + \sum_{m=1}^{M_{th}^{\tau}-1}\sum_{i\in B_{m}^{\tau}} P_{i,k,r}^{char}, \tag{26b}$$

$$part_{cons2}^{Cent} = \sum_{m=1}^{M_{th}^{\tau}}\sum_{i\in B_{m}^{\tau}} P_{i,k,r}^{char}\cdot x_{i,k,r}^{char}. \tag{26c}$$

According to $part_{cons1}^{Cent}$ and $part_{cons2}^{Cent}$, the obtained objective value of the centralized algorithm is expressed as

$$\max^{Cent} = \sum_{k=1}^{K}\sum_{i=1}^{\tilde{N}_{kr}} H_{i,k,r}^{char}\cdot x_{i,k,r}^{char} = part_{obj1}^{Cent} + part_{obj2}^{Cent}, \tag{27a}$$

$$part_{obj1}^{Cent} = \sum_{m=1}^{M_{th}^{1}-1}\sum_{i\in B_{m}^{1}} H_{i,k,r}^{char} + \sum_{m=1}^{M_{th}^{2}-1}\sum_{i\in B_{m}^{2}} H_{i,k,r}^{char} \cdots + \sum_{m=1}^{M_{th}^{\tau}-1}\sum_{i\in B_{m}^{\tau}} H_{i,k,r}^{char}, \tag{27b}$$

$$part_{obj2}^{Cent} = \sum_{m=1}^{M_{th}^{\tau}}\sum_{i\in B_{m}^{\tau}} H_{i,k,r}^{char}\cdot x_{i,k,r}^{char}. \tag{27c}$$

According to (18), if $M^{Buck} = M^{Cent}$, $(max_U^{\tau})^{Buck} = (max_U^{\tau})^{Cent}$, and $(min_U^{\tau})^{Buck} = (min_U^{\tau})^{Cent}$, we can obtain

$$B_m^{\tau} = B_{1,m}^{\tau} \cup B_{2,m}^{\tau} \cdots \cup B_{K,m}^{\tau}. \tag{28}$$

Hence, $part_{cons1}^{Buck} = part_{cons1}^{Cent}$, $part_{obj1}^{Buck} = part_{obj1}^{Cent}$.

As the number of recursion $\tau \to \tau^{max}$, the length of bucket $\left(max_U^{\tau} - min_U^{\tau}\right)/M^{\tau} \to \varepsilon$, the number of USEVs in bucket $N_{k,m}^{\tau} = \left|B_{k,m}^{\tau}\right| \to 1$. If $N_{M_{th}^{\tau}}^{\tau} = \left|B_{M_{th}^{\tau}}^{\tau}\right| = \sum N_{k,M_{th}^{\tau}}^{\tau} = 1$, it reflects that one more USEV cannot be allowed under power constraint in (6), i.e., $\tilde{P}_{ref} - sum_{DO}^{\tau^{max}} < P_{i,k,r}^{char}$. Hence, $part_{cons2}^{Buck} = part_{cons2}^{Cent}$. Otherwise, there exists a small optimality gap g, which is defined as

$$g = (part_{obj2}^{Cent} - part_{obj2}^{Buck})/\max^{Cent}. \tag{29}$$

REFERENCES

[1] Z. Ji and X. Huang, "Plug-in electric vehicle charging infrastructure deployment of China towards 2020: Policies, methodologies, and challenges," *Renew. Sustain. Energy Rev.*, vol. 90, pp. 710–727, Jul. 2018.
[2] Z. Xu, W. Su, Z. Hu, Y. Song, and H. Zhang, "A hierarchical framework for coordinated charging of plug-in electric vehicles in China," *IEEE Trans. Smart Grid*, vol. 7, no. 1, pp. 428–438, Jan. 2016.
[3] H. Zhang, S. J. Moura, Z. Hu, and Y. Song, "PEV fast-charging station siting and sizing on coupled transportation and power networks," *IEEE Trans. Smart Grid*, vol. 9, no. 4, pp. 2595–2605, Jul. 2018.
[4] B. Sun, Z. Huang, X. Q. Tan, and D. H. K. Tsang, "Optimal scheduling for electric vehicle charging with discrete charging levels in distribution grid," *IEEE Trans. Smart Grid*, vol. 9, no. 2, pp. 624–634, Apr. 2018.
[5] A. Malhotra, G. Binetti, A. Davoudi, and I. D. Schizas, "Distributed power profile tracking for heterogeneous charging of electric vehicles," *IEEE Trans. Smart Grid*, vol. 8, no. 5, pp. 2090–2099, Sep. 2017.
[6] J. Zhang, Y. Pei, J. Shen, L. Wang, and T. Ding, "Optimal charging strategy for electric vehicles using symbolic–graphic combination principle," *IET Gener., Transmiss. Distrib.*, vol. 13, no. 13, pp. 2761–2769, Jul. 2019.
[7] T. Ding, J. Bai, P. Du, B. Qin, F. Li, J. Ma, and Z. Dong, "Rectangle packing problem for battery charging dispatch considering uninterrupted discrete charging rate," *IEEE Trans. Power Syst.*, vol. 34, no. 3, pp. 2472–2475, May 2019.
[8] Y. Mu, J. Wu, N. Jenkins, H. Jia, and C. Wang, "A spatial–temporal model for grid impact analysis of plug-in electric vehicles," *Appl. Energy*, vol. 114, pp. 456–465, Feb. 2014.
[9] T. Shun, W. Jianfeng, X. Xiangning, Z. Jian, L. Kunyu, and Y. Yang, "Charging demand for electric vehicle based on stochastic analysis of trip chain," *IET Gener., Transmiss. Distrib.*, vol. 10, no. 11, pp. 2689–2698, Aug. 2016.
[10] D. Wang, J. Gao, P. Li, B. Wang, C. Zhang, and S. Saxena, "Modeling of plug-in electric vehicle travel patterns and charging load based on trip chain generation," *J. Power Sources*, vol. 359, pp. 468–479, Aug. 2017.
[11] L. Yu, T. Zhao, Q. Chen, and J. Zhang, "Centralized bi-level spatial-temporal coordination charging strategy for area electric vehicles," *CSEE J. Power Energy Syst.*, vol. 1, no. 4, pp. 74–83, Dec. 2015.
[12] M. Shepero and J. Munkhammar, "Spatial Markov chain model for electric vehicle charging in cities using geographical information system (GIS) data," *Appl. Energy*, vol. 231, pp. 1089–1099, Dec. 2018.
[13] M. B. Arias, M. Kim, and S. Bae, "Prediction of electric vehicle charging-power demand in realistic urban traffic networks," *Appl. Energy*, vol. 195, pp. 738–753, Jun. 2017.
[14] B. Hashemi, M. Shahabi, and P. Teimourzadeh-Baboli, "Stochastic-based optimal charging strategy for plug-in electric vehicles aggregator under incentive and regulatory policies of DSO," *IEEE Trans. Veh. Technol.*, vol. 68, no. 4, pp. 3234–3245, Apr. 2019.
[15] X. Dong, Y. Mu, H. Jia, J. Wu, and X. Yu, "Planning of fast EV charging stations on a round freeway," *IEEE Trans. Sustain. Energy*, vol. 7, no. 4, pp. 1452–1461, Oct. 2016.
[16] A. Pan, T. Zhao, H. Yu, and Y. Zhang, "Deploying public charging stations for electric taxis: A charging demand simulation embedded approach," *IEEE Access*, vol. 7, pp. 17412–17424, 2019.

[17] T. Yang, X. Xu, Q. Guo, L. Zhang, and H. Sun, "EV charging behaviour analysis and modelling based on mobile crowdsensing data," *IET Gener., Transmiss. Distrib.*, vol. 11, no. 7, pp. 1683–1691, May 2017.
[18] Y. Wang, W. Ding, L. Huang, Z. Wei, H. Liu, and J. A. Stankovic, "Toward urban electric taxi systems in smart cities: The battery swapping challenge," *IEEE Trans. Veh. Technol.*, vol. 67, no. 3, pp. 1946–1960, Mar. 2018.
[19] J. Fraile-Ardanuy, S. Castano-Solis, R. Álvaro-Hermana, J. Merino, and Á. Castillo, "Using mobility information to perform a feasibility study and the evaluation of spatio-temporal energy demanded by an electric taxi fleet," *Energy Convers. Manage.*, vol. 157, pp. 59–70, Feb. 2018.
[20] Y. Kim, J. Kwak, and S. Chong, "Dynamic pricing, scheduling, and energy management for profit maximization in PHEV charging stations," *IEEE Trans. Veh. Technol.*, vol. 66, no. 2, pp. 1011–1026, Feb. 2017.
[21] J. Tan and L. Wang, "Real-time charging navigation of electric vehicles to fast charging stations: A hierarchical game approach," *IEEE Trans. Smart Grid*, pp. 1–1, 2015.
[22] W. Yuan, J. Huang, and Y. J. Zhang, "Competitive charging station pricing for plug-in electric vehicles," *IEEE Trans. Smart Grid*, vol. 8, no. 2, pp. 627–639, Mar. 2015.
[23] W. Lee, L. Xiang, R. Schober, and V. W. S. Wong, "Electric vehicle charging stations with renewable power generators: A game theoretical analysis," *IEEE Trans. Smart Grid*, vol. 6, no. 2, pp. 608–617, Mar. 2015.
[24] Q. Guo, Y. Wang, H. Sun, Z. Li, and B. Zhang, "Research on architecture of ITS based smart charging guide system," in *Proc. IEEE Power Energy Soc. Gen. Meeting*, Detroit, MI, USA, Jul. 2011, pp. 1–5.
[25] Q. Guo, S. Xin, H. Sun, Z. Li, and B. Zhang, "Rapid-charging navigation of electric vehicles based on real-time power systems and traffic data," *IEEE Trans. Smart Grid*, vol. 5, no. 4, pp. 1969–1979, Jul. 2014.
[26] J.-Y. Yang, L.-D. Chou, and Y.-J. Chang, "Electric-vehicle navigation system based on power consumption," *IEEE Trans. Veh. Technol.*, vol. 65, no. 8, pp. 5930–5943, Aug. 2016.
[27] F. Xia, H. Chen, L. Chen, and X. Qin, "A hierarchical navigation strategy of EV fast charging based on dynamic scene," *IEEE Access*, vol. 7, pp. 29173–29184, 2019.
[28] H. Zhang, Z. Hu, and Y. Song, "Power and transport nexus: Routing electric vehicles to promote renewable power integration," *IEEE Trans. Smart Grid*, early access, Jan. 17, 2020, doi: 10.1109/TSG.2020.2967082.
[29] Z. Tian, T. Jung, Y. Wang, F. Zhang, L. Tu, C. Xu, C. Tian, and X.-Y. Li, "Real-time charging station recommendation system for electric-vehicle taxis," *IEEE Trans. Intell. Transp. Syst.*, vol. 17, no. 11, pp. 3098–3109, Nov. 2016.
[30] C.-K. Wen, J.-C. Chen, J.-H. Teng, and P. Ting, "Decentralized plug-in electric vehicle charging selection algorithm in power systems," *IEEE Trans. Smart Grid*, vol. 3, no. 4, pp. 1779–1789, Dec. 2012.

JIALEI ZHANG (Member, IEEE) received the B.S. and M.S. degrees from the Xi'an University of Technology, Xi'an, China, in 2010 and 2013, respectively. She is currently pursuing the Ph.D. degree with School of Electrical Engineering at Xi'an Jiaotong University, Xi'an.

Since 2013, she has been a Lecturer with the Department of Electric Power Engineering, Shanxi University, Taiyuan, China. Her research interests include demand response, energy storage systems, and vehicle-to-grid control.

YUNQING PEI (Member, IEEE) was born in 1969. He received the B.S. and M.S. degrees in electrical engineering and the Ph.D. degree in power electronics from Xi'an Jiaotong University, Xi'an, China, in 1991, 1994, and 1999, respectively. He then became a Faculty Member with Xi'an Jiaotong University, where he is currently a Professor. From February 2006 to February 2007, he was a Visiting Scholar with the Center of Power Electronics Systems, Virginia Polytechnic Institute and State University, Blacksburg, VA, USA. His research interests include high-power inverters, switch-mode power supply, and converters in distributed generation systems.

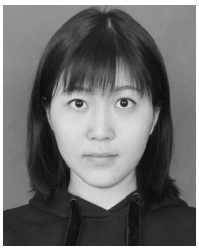

JIAMING SHEN (Student Member, IEEE) received the B.S. degree from Xi'an Jiaotong University, China, in 2017, where she is currently pursuing the Ph.D. degree. Her research interests include electric vehicle control, energy storage systems, and microgrid operation control.

LAILI WANG (Senior Member, IEEE) was born in Shaanxi, China, in 1982. He received the B.S., M.S., and Ph.D. degrees in electrical engineering from Xi'an Jiaotong University, Xi'an, China, in 2004, 2007, and 2011, respectively. Since 2011, he has been a Postdoctoral Research Fellow with the Electrical Engineering Department, Queen's University, Kingston, ON, Canada. From 2014 to 2017, he was an Electrical Engineer with Sumida, Kingston. In 2017, he joined Xi'an Jiaotong University, as a Professor. His research interests include package and integration of passive devices in high-frequency high power density dc/dc converters, wireless power transfer, and energy harvesting.

TAO DING (Senior Member, IEEE) received the B.S.E.E. and M.S.E.E. degrees from Southeast University, Nanjing, China, in 2009 and 2012, respectively, and the Ph.D. degree from Tsinghua University, Beijing, China, in 2015. He was a Visiting Scholar with the Department of Electrical Engineering and Computer Science, The University of Tennessee, Knoxville, TN, USA. He is currently an Associate Professor with the State Key Laboratory of Electrical Insulation and Power Equipment, School of Electrical Engineering, Xi'an Jiaotong University, Xi'an, China. He has authored or coauthored more than 60 technical articles and authored by "Springer Theses" recognizing outstanding Ph.D. research around the world and across the physical sciences-power system operation with large-scale stochastic wind power integration. His current research interests include electricity markets, power system economics and optimization methods, and power system planning and reliability evaluation.

SEN WANG (Graduate Student Member, IEEE) received the B.S. and M.S. degrees from the School of Electrical Engineering, Xi'an University of Technology, Xi'an, China, in 2009 and 2012, respectively. He is currently pursuing the Ph.D. degree with the Power Electronics and Renewable Energy Research Center, Xi'an Jiaotong University. His current research interests include power conversion systems, harmonics suppression, reactive power compensation, and active power filters.